





# Ecohydrological modelling with ECH<sub>2</sub>O-iso to quantify forest and grassland effects on water partitioning and flux ages

Audrey Douinot<sup>1</sup>  | Doerthe Tetzlaff<sup>1,2,3</sup>  | Marco Maneta<sup>4</sup> | Sylvain Kuppel<sup>3</sup>  | Hubert Schulte-Bisping<sup>5</sup> | Chris Soulsby<sup>1,3</sup> 

<sup>1</sup>Department of Hydroecology, Leibniz Institute of Freshwater Ecology and Inland Fisheries, Berlin, Germany

<sup>2</sup>Department of Geography, Humboldt University of Berlin, Berlin, Germany

<sup>3</sup>Northern Rivers Institute, University of Aberdeen, Aberdeen, UK

<sup>4</sup>Geosciences Department, University of Montana, Missoula, Montana

<sup>5</sup>Soil Science of Temperate Ecosystems, BÜSgen-Institute, Göttingen, Germany

## Correspondence

Audrey Douinot, Department of Hydroecology, Leibniz Institute of Freshwater Ecology and Inland Fisheries, Berlin 12587, Germany.

Email: audreydouinot@gmail.com

## Funding information

FP7 Ideas: European Research Council, Grant/Award Number: GA 335910 VeWa; U. S. National Science Foundation, Grant/Award Number: GSS 1461576

## Abstract

We used the new process-based, tracer-aided ecohydrological model ECH<sub>2</sub>O-iso to assess the effects of vegetation cover on water balance partitioning and associated flux ages under temperate deciduous beech forest (F) and grassland (G) at an intensively monitored site in Northern Germany. Unique, multicriteria calibration, based on measured components of energy balance, hydrological function and biomass accumulation, resulted in good simulations reproducing measured soil surface temperatures, soil water content, transpiration, and biomass production. Model results showed the forest “used” more water than the grassland; of 620 mm average annual precipitation, losses were higher through interception (29% under F, 16% for G) and combined soil evaporation and transpiration (59% F, 47% G). Consequently, groundwater (GW) recharge was enhanced under grassland at 37% (~225 mm) of precipitation compared with 12% (~73 mm) for forest. The model tracked the ages of water in different storage compartments and associated fluxes. In shallow soil horizons, the average ages of soil water fluxes and evaporation were similar in both plots (~1.5 months), though transpiration and GW recharge were older under forest (~6 months compared with ~3 months for transpiration, and ~12 months compared with ~10 months for GW). Flux tracking using measured chloride data as a conservative tracer provided independent support for the modelling results, though highlighted effects of uncertainties in forest partitioning of evaporation and transpiration. By tracking storage–flux–age interactions under different land covers, ECH<sub>2</sub>O-iso could quantify the effects of vegetation on water partitioning and age distributions. Given the likelihood of drier, warmer summers, such models can help assess the implications of land use for water resource availability to inform debates over building landscape resilience to climate change. Better conceptualization of soil water mixing processes and improved calibration data on leaf area index and root distribution appear obvious respective modelling and data needs for improved simulations.

## KEYWORDS

forest hydrology, ecohydrology, tracers, tracer-aided models

This is an open access article under the terms of the Creative Commons Attribution License, which permits use, distribution and reproduction in any medium, provided the original work is properly cited.

© 2019 The Authors Hydrological Processes Published by John Wiley & Sons Ltd

## 1 | INTRODUCTION

Vegetation exerts a strong control on land-surface water and energy partitioning, and the resulting ecohydrological fluxes of “green water” as evaporation and transpiration (Baldocchi, Xu, & Kiang, 2004; Llorens & Domingo, 2007; Villegas et al., 2015; Wang, Good, & Caylor, 2014), and the residual “blue water” fluxes to groundwater recharge and run-off (Jencso & McGlynn, 2011; Williams et al., 2012). Thus, it is well established that forests generally “use” more water than grass or short crops due to higher evapotranspiration (Fatichi, Pappas, & Ivanov, 2016). However, there are strong codependencies between plant growth, seasonal phenological change and life cycles, and the physical processes that drive water movement that we poorly understand (Jolly & Running, 2004; Porporato, Laio, Ridolfi, & Rodriguez-Iturbe, 2001; Wang, Tetzlaff, Dick, & Soulsby, 2017). Elucidating these interactions is an essential prerequisite for modelling the hydrological effects of land cover change and their ecological implications and for mitigating the negative impacts that it may have, including effects on climate at local, regional, and global scales. Thus, although it is well known that conversion of natural forest to agriculture generally reapporitions “green” and “blue” water fluxes, in the direction of increasing run-off, intensifying downstream flood risk and enhancing baseflows; the effects are usually site specific depending on hydroclimate and biogeography (Amogu et al., 2015; Archer, 2007; García-Ruiz et al., 2008). In addition, climate change predictions generally indicate higher future atmospheric water demands in temperate regions, as well as seasonal redistribution of rainfall with potentially drier summers (Trenberth et al., 2007). Within this context of growing climatic stress, the hydrological implications of land cover change on water partitioning and water availability are of increasing concern (Frei, Schöll, Fukutome, Schmidli, & Vidale, 2006; Nikulin, Kjellström, Hansson, Strandberg, & Ullerstig, 2011). Linked to this, in many areas, the natural response of vegetation communities to climate change is already being observed (Menzel et al., 2006), and this may also have important hydrological impacts (Tetzlaff et al., 2013).

Yet despite the long history of research into land cover change effects on hydrology, many details of the role of vegetation in regulating water partitioning are difficult to quantify (Zhang, Yang, Yang, & Jayawardena, 2016). For example, the impacts of vegetation dynamics on water fluxes—in terms of directional long-term growth and seasonal phenology—are rarely well constrained (Huisman et al., 2009). Historically, most hydrological models conceptualize vegetation as a static element with prescribed constants that parameterize the physical processes of evapotranspiration, disregarding the strong coupling between evapotranspiration and the physiological processes that drive plant phenology and water use (Fatichi et al., 2016; Speich, Lischke, Scherstjanoi, & Zappa, 2016; Wegehenkel, 2009). Over the past 15 years, various ecohydrological models have explicitly included dynamic vegetation parameterization to overcome such limitations (e.g., RheSYSS [Tague & Band, 2004], EcH<sub>2</sub>O [Maneta & Silverman, 2013; Kuppel, Tetzlaff, Maneta, & Soulsby, 2018a; Simeone et al., 2019], tRIBS-VEGGIE [Ivanov, Bras, & Vivoni, 2008], Cathy [Niu et al., 2014], Tethys-Chloris [Fatichi, Ivanov, & Caporali, 2012], and

FLETCH2 [Mirfenderesgi et al., 2016]). However, the verification of these models is often focused on short-term to midterm hydrologic (e.g., streamflows and soil moisture) and ecological dynamics (e.g., seasonal phenology), and rarely are these models compared with long-term direct metrics of vegetation dynamics (e.g., biomass production and transpiration) that affect the water balance.

Along with advances in ecohydrological modelling, experimental studies using water isotopes and other conservative tracers have advanced our understanding of how water flows in catchments, and helped improve how hydrological models represent the celerity of hydrological fluxes, as well as the velocity of water particles and the mixing relationships within soils (McGuire & McDonnell, 2006; Birkel, Soulsby, & Tetzlaff, 2011; Peters, Burns, & Aulenbach, 2014; Klaus, Chun, McGuire, & McDonnell, 2015; Benettin, Kirchner, Rinaldo, & Botter, 2015; Sprenger, Tetzlaff, Buttle, Carey, et al., 2018). Such tracer-aided models can also track the age distributions of water in different catchment storage compartments and “green” and “blue” water fluxes (Soulsby et al., 2015; van Huijgevoort, Tetzlaff, Sutanudjaja, & Soulsby, 2016; Remondi, Kirchner, Burlando, & Fatichi, 2018). Recent work has shown that when integrated with explicit representation of vegetation dynamics, these tracer-aided modelling concepts are better positioned to assess the interactions of plants and water partitioning in response to hydroclimatic variability because they can help determine the pools of water that plant use and how they affect water mixing, hydrologic connectivity, and the establishment of flow paths (Kuppel, Tetzlaff, Maneta, & Soulsby, 2018b). In conjunction with tracer data, such models can provide insight into the fate of soil water and the processes that determine the ecohydrological separation of “green” fluxes that sustain biomass and “blue” water fluxes that sustain groundwater recharge and stream flow generation (Evaristo, Jasechko, & McDonnell, 2015; McDonnell, 2014; Sprenger, Tetzlaff, Buttle, Laudon, et al., 2018).

In this study, we apply the process-based, tracer-aided ecohydrological model, EcH<sub>2</sub>O-iso (Kuppel et al., 2018b), to quantify the contrasting effects of seminatural forest and grassland on water partitioning and flux ages at an intensively studied site in Northern Germany. The data-rich nature of the site provided measurements of energy balance components (through a fully automated weather station), hydrological processes (precipitation, throughfall, transpiration, soil moisture, and groundwater levels) and biomass production (litterfall and forest growth metrics). The study site at Stechlin is located in the German state of Brandenburg, which is drought-sensitive, and is an extensively forested area where there is concern over land use effects on groundwater recharge; in particular, the role of forest management for timber production in reducing recharge. This is compounded by climate change predictions, which forecast warmer and drier summers (Dorau, Gelhausen, Esplör, & Mansfeldt, 2015; Lischke & Nathkin, 2011; Riediger, Breckling, Svoboda, & Schröder, 2016). Thus, we aim to show how multiproxy data can be used to improve the robustness of quantifying land use effects on the water balance using an ecohydrological model. This is done with the anticipation that such advances will help inform land use strategies designed to build landscape resilience to climate change and protect water resource needs. The specific objectives are the following:

1. To conduct a multicriteria calibration of ECH<sub>2</sub>O-iso for concurrent energy balance, water balance, and biomass production simulations.
2. To quantify, within an uncertainty framework, the role of forest and grassland vegetation on the local water balance in terms of water partitioning and ages of different vertical fluxes.
3. To use tracers to test the internal consistency of the model and implications for interpreting the resulting age distributions of different fluxes.
4. To assess the implications of future land management, in the context of climate change, for water partitioning and water availability.

The context of the modelling was also to use ECH<sub>2</sub>O-iso in a learning framework to understand how to both improve the model and prioritize data collection for future studies.

## 2 | STUDY SITE AND DATA

### 2.1 | Site description

Two long-term study plots are located in the catchment of the extensively monitored Lake Stechlin (Bergström et al., 2003; Casper, 2012; Dieffenbach-Fries, Hofmann, & Schleyer, 2003); a groundwater-sourced lake in the headwaters of the River Havel in Northern Germany (53°08'N, 13°02'E; Figure 1). The region has a temperate, continental climate with strong seasonality, and significant interannual variability in net radiation and temperatures (Figure 2a). Average annual precipitation is 620 mm, ranging between 400 and 820 mm

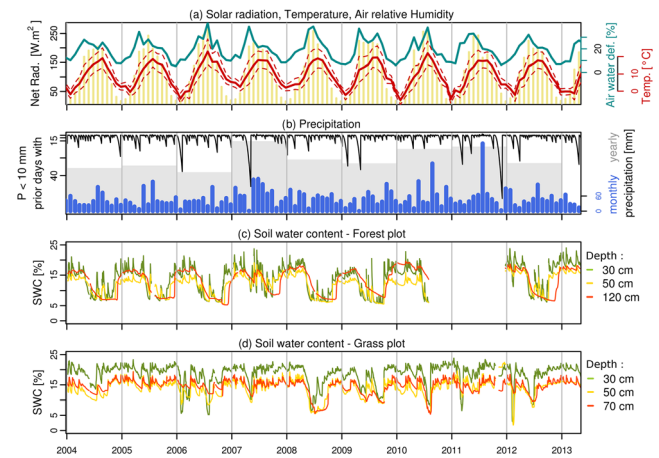


**FIGURE 2** (a) Main hydroclimatic data plotted at monthly time steps: Net solar radiation (yellow), monthly average of daily minimum, maximum and average temperature (red dashed and solid lines), and monthly average of the air water deficit (blue cyan line); (b) precipitation time series: number of prior days with less than 10 mm precipitation (black line) and monthly and yearly accumulation (blue hystograms and grey polygons); daily soil water content (c) in the forest and (d) grass plots

year<sup>-1</sup> during the 2000–2014 period (Figure 2b). Precipitation is relatively evenly distributed, with peaks when frontal rain dominates in winter, and convective rain falls in summer. Average annual potential evapotranspiration (PET), estimated using the Thornthwaite equation is 645 mm, ranging between 620 and 670 mm year<sup>-1</sup> during the 2000–2014 period (Thornthwaite, 1948). The dominant land cover in the area is >100-year-old seminatural mixed deciduous/conifer forest, which is managed for conservation purposes. In the forest study plot,

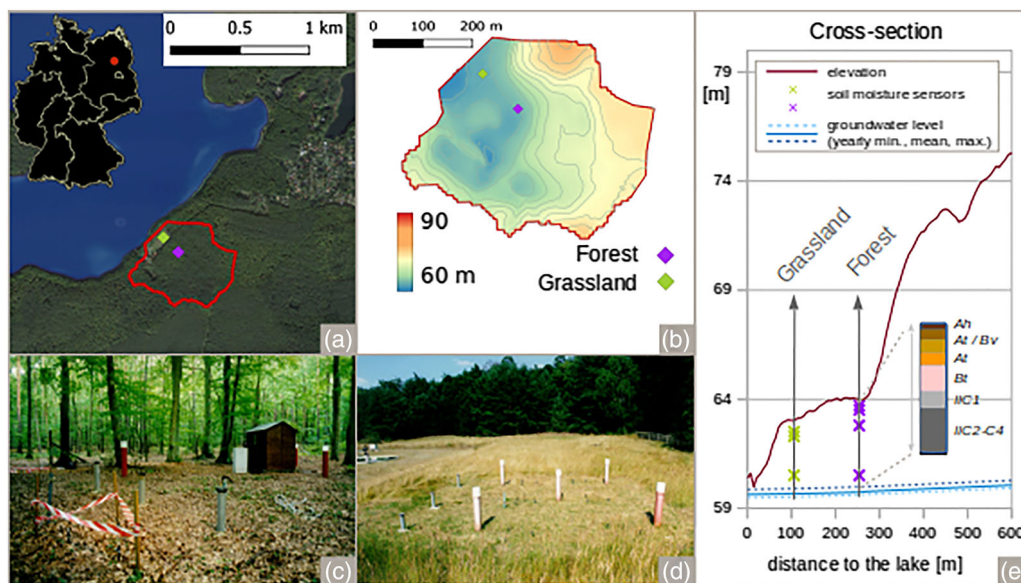


**FIGURE 1** Study site location of the two monitoring plots in Northern Germany and aerial view of edge of Lake Stechlin (a), the topography (b), view of the forest (c) and grassland plots (d), and schematic profile section of ground surface elevation, soil profile characteristics (the soil horizons are defined according to the USDA taxonomy: a–c are the surface, illuvial, and little-altered substrate horizons, respectively; the suffixes h, t, and v refer to organic rich, clay translocation, and iron deposition, respectively), water table depth and instrumentation depths (e). Photos (c) and (d) from Brüning, Graf, & Nützmann, 2003

this is mostly composed of deciduous beech (*Fagus sylvatica*, >80%) trees and also some Scots pine (*Pinus sylvestris*; Table 1; Schulte-Bisping, Beese, & Dieffenbach-Fries, 2012). The second plot is perennial semidry grassland dominated by a dense sward of *Calamagrostis epigejos*, *Festuca ovina*, and *Koeleria glauca*, which is cut (similar to a cut or grazed meadow) to facilitate access to the instrumentation (Figure 1). This is typical grassland vegetation after forest removal and a grazing management regime.

The plots are in a lowland area (~65-m elevation) with a gentle slope (median = 4.5%). The lake and low-lying topography were formed at the end of the Weichselian glacial period, with extensive drift deposits covering the solid geology (Merz & Pekdeger, 2011). The upper unconfined aquifer (up to 50 m thick) consists of permeable sandy glacial outwash sediments (hydraulic conductivity  $K \sim 10^{-4} \text{ m s}^{-1}$ ; Richter, 1997; Ginzel & Kaboth, 1999; Samek, 2000). At the plots, the water table lies around 5–6 m below the soil surface with limited seasonal variability (manifest as a small [ $<0.3 \text{ m}$ ] winter rise), probably related to the boundary control of the lake's surface elevation.

The study plots overlie these drift deposits, with freely draining, weakly podzolized sandy soils classified as haplic arenosols. These are >1 m deep with a 30 cm deep organic-rich A horizon overlying the mineral B and C horizons in the subsoil (Figure 1e). In both soils, rooting densities are the highest in the upper 30 cm, though in the forest deeper roots can reach down below 1 m. The soils are dominated by vertical drainage due to the high hydraulic conductivity and flat topography. In both plots, the soil moisture content (measured with time-domain reflectometry [TDR] probes—see below) exhibits seasonality, which is particularly pronounced at the forest site (Figure 2c,d). The upper 30 cm, with the highest organic content, is the wettest, with the volumetric soil moisture content varying between ~22% when wet and ~5% when dry. Wet periods are transient during and immediately after high rainfall. Soil moisture content in the minerogenic subsoil (at and below 50 cm) similarly varies between ~7% and ~20%. Here, at the forest site, a strong, general pattern of winter wetting and summer drying mostly dominates shorter term variability, whereas in the grassland plot, short-term patterns of wetting and drying are stronger throughout the profile. Soil moisture regimes can show marked interannual variability, with large, prolonged deficits in dry years such as 2008, and limited summer deficits in wet years such as 2007.

## 2.2 | Available data

The plots form part of long-term environmental monitoring at Stechlin (Bergström et al., 2003; Casper, 2012; Dieffenbach-Fries et al., 2003;

**TABLE 1** Vegetation properties of the forest plot (Schulte-Bisping & Beese, 2012): data are global or species-specific beech (°) or pine (\*\*) characteristics

Stem density (tree ha <sup>-1</sup> )	Sapwood area (m <sup>2</sup> ha <sup>-1</sup> )	Age (year)	Height (m)	Albedo (-)	Root depth (m)
296	20.5°/8.5**	100°/150**	29°/34**	0.1	>2

Pöschke, Nützmann, Engesgaard, & Lewandowski, 2018) and are linked to a network of pan-European sites for assessing the ecosystems effects of acid deposition (Tørseth et al., 2012; Fagerli & Aas, 2008). Consequently, a wide range of data is available for ecohydrological modelling (Figure 3). Long-term hourly climate observations (precipitation, temperature, incoming short-wave radiation, outgoing long-wave radiation, relative humidity, wind speed, etc.) have been measured adjacent to the grassland plot since 1950. Soil properties have been characterized, and soil moisture has been monitored since 2000 (Nützmann, Holzbecher, & Pekdeger, 2003). TDR probes were installed in 2004 at four depths (three replicates) at both plots: 30, 50, 70, and 250 cm at the grassland and 30, 50, 120, and 350 cm at the forest. In the latter part of the study, soil temperatures (from the TDR probes) have also been monitored. Technical problems prevented data collection at the forest plot for a just over a year between 2010 and 2011.

At the forest plot, biomass measurements related to seasonal and long-term tree growth dynamics are available. Litterfall was measured between 2004 and 2009, allowing an annual assessment of leaf, needle, and fruit production. Stem diameters of 12 representative trees were measured during the same period using dendrometer bands. Using the tree volume equations of Bergel (1973), this provides a first approximation of the above-ground biomass accumulation. Unfortunately, equivalent biomass data were not available for the grassland. The minimum and maximum leaf area index (LAI) were estimated through undercanopy transmittance measurements using the SunScan Type SS1 from Delta-T device, in January and August 2005 under beech trees. In addition, hourly sap flow of six beech trees and five pines was measured during the 2013 growing season with thermal dissipation probes. These were weighted according to species cover and upscaled to an estimate of plot transpiration after sampling trees to assess the sapwood area in the study plot. In addition to the in situ measurements, we used incoming short-wave solar radiation and down-welling long-wave radiation (required as model inputs) from the online ERA-Interim climate reanalysis source (Dee et al., 2011).

Finally, the overall rich and varied data set provides multidimensional information related to water balance, energy distribution or vegetation dynamics facilitating a multicriteria calibration and/or validation of the ECH<sub>2</sub>O-iso model similar to Kuppel et al. (2018a); Figure 3).

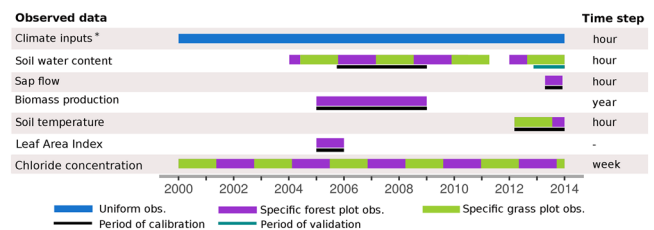


**FIGURE 3** Summary of the data sets available at the two plots: time series periods and time step resolution. Climate inputs comprise daily time series of incoming short-wave solar radiation and down-welling long-wave radiation; minimum, average and maximum temperature, precipitation, air relative humidity, wind speed

The chemical composition of rainfall, forest throughfall (15 rainfall collectors arranged in a cruciform pattern in the forest plot) and soil waters (using suction lysimeters at depths of 30, 50, 70, and 250 cm at the grassland and 30, 50, 120, and 350 cm at the forest) has also been monitored by sampling at approximately biweekly intervals. As an independent check on how well  $\text{EcH}_2\text{O}$ -iso captures interactions between water storage, flux dynamics, and associated mixing relationships, we used the chloride data collected from precipitation, throughfall and soil water as an assumed conservative tracer in the model for the forest site (cf. Peters & Ratcliffe, 1998). This was not possible at the grassland site as concentrations were too low and uncertainties too high in the absence of monitoring of throughfall and the effects of dry and occult deposition on the grass sward.

### 3 | $\text{EcH}_2\text{O}$ -ISO DESCRIPTION AND PARAMETERIZATION

#### 3.1 | Description of $\text{EcH}_2\text{O}$ -iso 1.0

$\text{EcH}_2\text{O}$  is a spatially distributed, process-based ecohydrological model (Figure 4) that simulates: (a) the energy balance over a two-layer (canopy and understorey) vegetation system; (b) vertical and lateral water fluxes for the surface and subsurface (conceptualized in three soil layers corresponding to the near-surface, vadose, and saturated zones); and (c) vegetation dynamics through a transpiration-based simulator of carbon uptake and allocation for plant growth (Lozano-Parra, Maneta, & Schnabel, 2014; Maneta & Silverman, 2013).  $\text{EcH}_2\text{O}$ -iso extends the original model with a component for tracking the isotopic signature of the water storage compartments and computing the ages of associated fluxes (Kuppel et al., 2018b). In this study, we further adapt the model formulation to simulate other passive tracers, such as chloride, which are not subject to evaporative fractionation but evapoconcentration. This flux tracking assumes complete mixing in each storage compartment such that they can be defined by a single average concentration and age, with no preferential age or concentration selection by the water fluxes. Under these assumptions, the concentration and age of outgoing fluxes at each time step correspond to those of the storage compartment at that time.

We used  $\text{EcH}_2\text{O}$ -iso to model the interlinkages between energy balance, water cycling, and biomass production and quantify the effects on water partitioning and water ages at the Stechlin site. Past studies have successfully applied the model in different environments at the watershed scale (Kuppel et al., 2018a; Lozano-Parra et al., 2014). This study provides an application of the model at the grid-cell scale to resolve and track the age of “green” and “blue” water fluxes. For the forest plot, measurements of tree biomass production also enabled us to explicitly include in the model calibration process metrics of daily, seasonal, and/or long-term plant physiological dynamics (stem and leaf growth, transpiration, canopy cover, etc.), along with more commonly used observations pertinent to the energy (e.g., soil temperatures) and water balance (e.g., soil moisture) components. Additionally, we used the chloride time series in precipitation,

throughfall and soil water as independent (i.e., not used for calibration) tracers of water fluxes for model verification.

At each time step (daily in this application), the model requires meteorological information of incoming short-wave radiation ( $R_{\text{SW}}$ ), down-welling long-wave radiation ( $R_{\text{LW}}$ ), air temperature (maximum  $T_{\text{a,max}}$ , minimum  $T_{\text{a,min}}$ , and average  $T_{\text{a,mean}}$ ), wind speed (Ws), and relative humidity ( $H_r$ ). Canopy and surface temperatures are used to resolve the balance between available radiative energy (net radiation) and turbulent energy fluxes (sensible, latent, ground heat, and heat into the snowpack) using the Newton–Raphson method. The canopy layer can include different vegetation covers (including bare soil) within each grid cell. Canopy dynamics and seasonal variations of LAI feedback into the energy balance through its controls on canopy conductance, aerodynamic conductance, vertical attenuation of momentum, light interception, and variation in the maximum water storage capacity.

The energy balance computes the energy expended in evaporation and transpiration. Main components of the water balance in the vertical soil-vegetation column include canopy interception, snowpack, surface ponding storage, and three soil layers (Figure 4b). Vertical water fluxes are driven by gravitational gradients (diffusive effects are assumed to be negligible). Water infiltration into the first soil layer is simulated using the Green and Ampt equation (Mays, 2010). Evaporation is limited to this upper layer. Drainage from the upper soil layers to deeper layers occurs when field capacity is exceeded, the rate of percolation increasing linearly with the water content of the source layer. Leakance through the bottom boundary of the soil follows the same approach, but the rate is further controlled by a leakance parameter to represent the condition range between free drainage and no drainage (i.e., water tight bedrock).

The distribution of soil water losses from transpiration uptake is determined from the fraction of roots present in each soil layer. Simulation of carbon uptake and plant growth is adapted from the 3-PG (Landsberg & Waring, 1997) and TREEDYN3 models (Bossel, 1996; Peng, Liu, Dang, Apps, & Jiang, 2002). Gross and net primary production (GPP and NPP) are calculated using a multiplicative function of the photosynthetically active radiation and the amount of transpired water (Figure 4c). Carbon allocation and growth routines are different for herbaceous vegetation and trees; the former having only two carbon pools (leaves and roots; Lozano-Parra et al., 2014; Istanbuloglu, Wang, & Wedin, 2012), whereas trees have three (leaves, roots, and stems). For the study site, we had direct measurements of annual leaf production and stem biomass accumulation to help calibrate the model (see above).

#### 3.2 | Model set-up

##### 3.2.1 | Approach to calibration

In  $\text{EcH}_2\text{O}$ -iso, we used multicriteria calibration involving diagnostic metrics of model performance in each of the energy, water, and vegetation dynamic modules (Kuppel et al., 2018a). At the data-rich Stechlin site, we adopted this approach to assess the model skill at

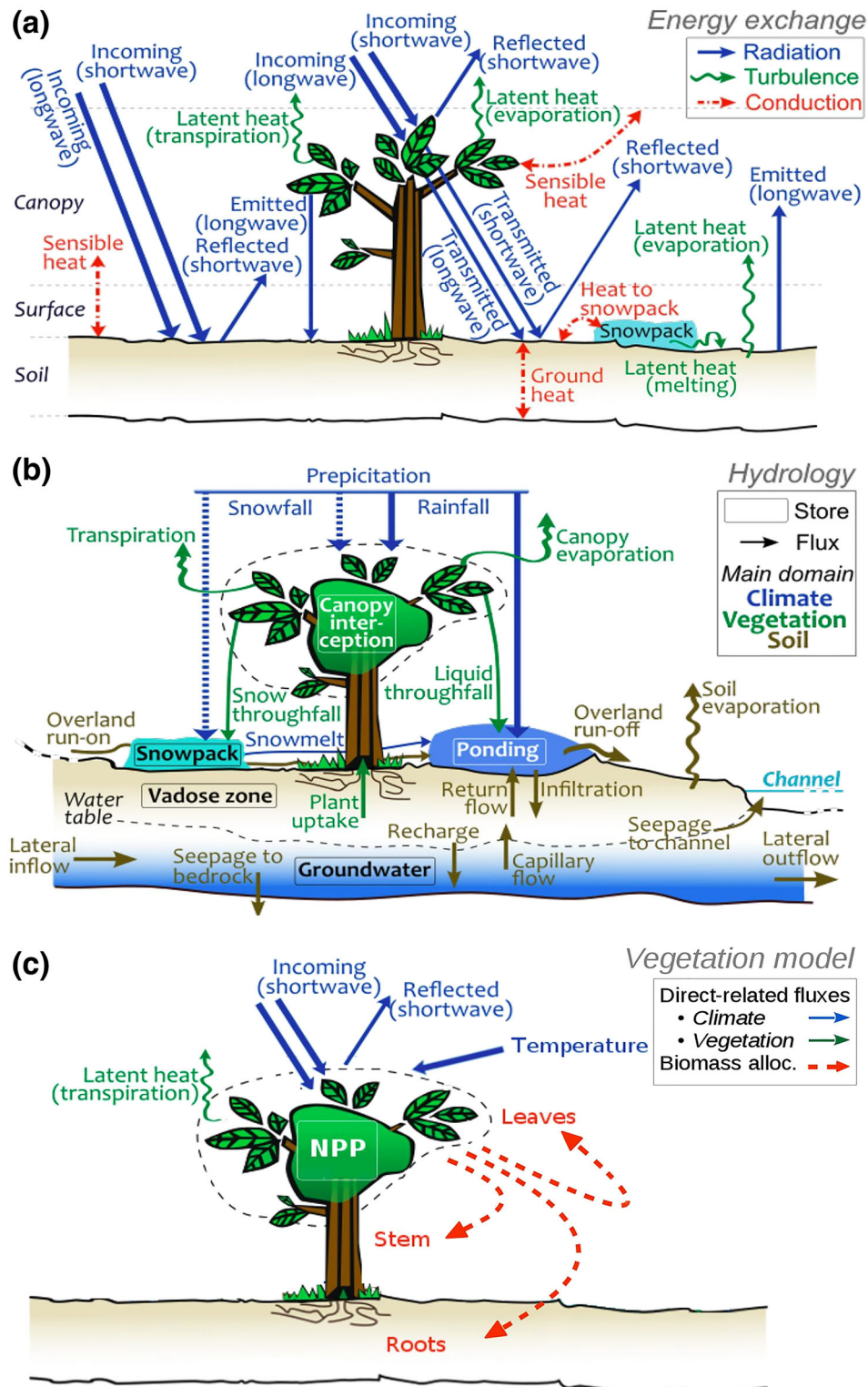


**FIGURE 4** Schematic of the processes simulated in (a) the energy balance, (b) the hydrologic, and (c) the vegetation modules of the ECH<sub>2</sub>O model (adapted from Kuppel et al., 2018a)

reproducing the dynamics of different ecohydrological data sets using long-term, seasonal, and daily periods. We used a range of metrics to determine which parameter sets are “acceptable” or “behavioural” (Beven, 2006; Beven & Binley, 1992). The criteria of the calibration are summarized in Table 2, and the time periods are used for each data

set in Figure 3. We used the multicriteria calibration to tune the model at daily time steps using dynamics of soil water content (SWC) at several soil depths and soil surface temperature for both plots. We chose the Kling–Gupta efficiency (KGE) statistic (Gupta et al., 2009) as our metric of “goodness of fit” for time series simulations. This equally

**TABLE 2** Summary of the criteria used to calibrate the model over the multiinformation data set

		Forest plot	Grassland plot
1. Dynamic assessment	Soil water content in the three layers	KGE over normalized TS	
	Soil surface temperature	KGE	
	Transpiration rate	KGE over normalized TS	
	Leaf area index	RMSE over the December–March and June–September periods	No data
2. Thresholds as limit of acceptability	Transpiration rate	Transpiration rate < basal sapflow measurements	No data
	LAI	Max (LAI) < 8	Max (LAI) < 5
	Biomass production	Stem growth, leaves production < 0.5 RMSE	NPP <sub>Grass</sub> < 0.75 max (NPP <sub>forest</sub> )
	Soil recharge	> 200 mm over 10 years	

Note. KGE, Kling-Gupta efficiency (Gupta, Kling, Yilmaz, & Martinez, 2009); LAI, leaf area index; NPP, net primary production; RMSE, root mean square error; TS, time series.

considers bias (through assessment of the mean), correlation (assessment of the timing), and variability (assessment of the range of variation). Additionally, measurements of LAI, stem growth, and transpiration rates were used for calibrating the forest plot (Table 2).

We also used various known quantitative thresholds as “observation-driven and expert-knowledge-based constraints” (Kelleher, McGlynn, & Wagener, 2017; Table 2). For example, previous water balance studies of Lake Stechlin (e.g., Pöschke et al., 2018) have estimated that the annual average groundwater recharge over the catchment (15 km<sup>2</sup>) ranges between 65 and 150 mm year<sup>-1</sup>, which is mainly covered by separate or mixed stands of beech and pine (97%; CORINE Land Cover database CLC 2012). Therefore, a minimal recharge threshold of 20 mm year<sup>-1</sup> averaged over the 2004–2014 simulation period was used as a limit to “behavioural” simulations. Similarly, a threshold on the maximum calibrated LAI for both plots was used for consistency with measured values for the forest site and literature value for the grassland (see Supporting Information). Daily transpiration rates in the forest plot were also limited by an upper threshold of the highest pine and beech transpiration rates reported in the literature. Finally, biomass production in the forest plot was constrained by requiring simulated leaf losses and stem growth to be within 50% of the observed values. In order, to maintain consistency between the forest and grassland simulations, the NPP of the grass plot was limited relative to the forest assuming an upper threshold of 0.75 of the maximum NPP simulated in the forest plot (Chapin, Matson, & Vitousek, 2011).

For the final multicriteria calibration, we used a Monte Carlo analysis with 30,000 runs. The quantitative assessment using thresholds was used to reject implausible simulations, whereas the dynamic assessment was used to rank the retained parameter sets according to their likelihood. A global score for each simulation ( $GS_i$ ) was calculated as follows:

$$GS_i = \sum_{v=1:n} \frac{LS_i^v}{\sigma(LS^v)}$$

where  $LS_i^v$  is the variable-specific assessment or “local” score of simulation  $i$  (KGE or RMSE; see Table 2) and  $\sigma(LS^v)$  the standard deviation of  $LS^v$  over the 30,000 runs. The latter standardization aimed to derive

a simple weight balancing of the variable-specific assessments when calculating the GS. The GS was finally used to select the 15 best simulations out of the likelihood simulations.

### 3.2.2 | Parameterization and sensitivity

As a preliminary step to model calibration, an analysis of parameter sensitivity was conducted to reduce the number of free parameters: any parameter, showing neither first nor second order sensitivity related to one of the LS, was removed from calibration parameter set and fixed to a value according to locally measured properties or to literature values. Table S1 presents the constant values prescribed to the parameters not included in the calibration set. The first and the second order parameter sensitivities were assessed on the basis of an ensemble of 30,000 Monte Carlo runs (Figures S2 and S3). A parameter was considered to have 1st order sensitivity according to an LS if the average parameter values of the 15,000 first runs, ranked using the LS values, differs from the average parameter values of the remaining 15,000 runs (t test with a significance of  $p < .01$ ). A parameter was considered to have second order sensitivity according to an LS if the parameter values of the 15,000 first runs are correlated with any other parameter, similarly selected ( $p$  values < .001). The final calibration set contained 26 parameters in the forest plot model and 21 parameters in the grassland plot model. Tables S2 and S3 show the calibrated soil and the vegetation parameters and their prior and posterior range of values.

## 4 | MODEL RESULTS

### 4.1 | Overall model performance

The performance metrics indicated that the model captures the dynamics of each target variable reasonably well (Figure 5). The RMSE (MAE) is lower than 26% (21%) for all the local scores, except the transpiration rate, though the Pearson correlation coefficient shows transpiration dynamics are captured reasonably well. For other variables, the Pearson coefficients of local calibrations were generally >0.75.

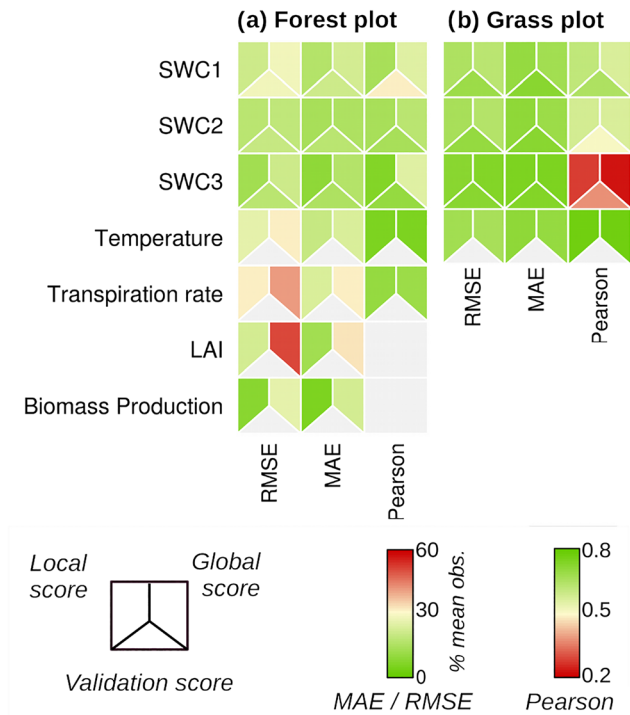


**FIGURE 5** Overview of the performance metrics obtained after calibration of the modelling results in the forest (a) and grass plot (b): root mean square error (RMSE), mean absolute error (MAE), Pearson coefficient, using (1) the specific score for local variables, (2) the final multicriteria GS scores over the calibration period, or (3) over the validation period (blue period; Figure 3); 50th percentile of the 15 best simulations

An exception is the SWC of the third layer of the grassland plot where measured variability is low (see below and Figure 2).

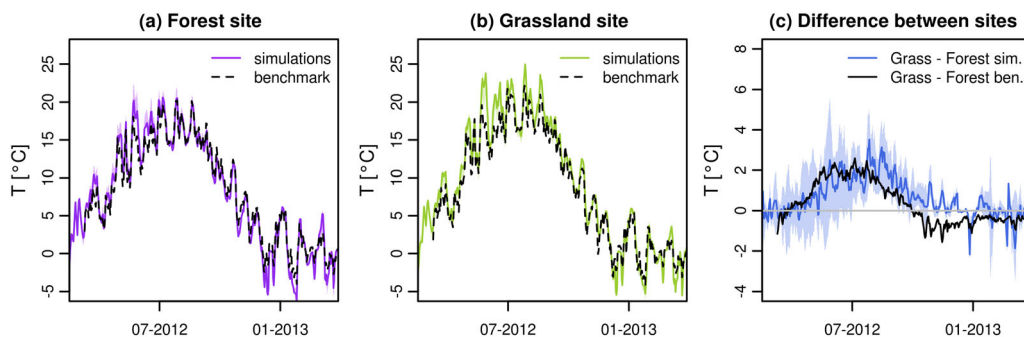
When the model is calibrated against all data sets simultaneously (global calibration), there is an expected overall decrease in the model performance compared with the performance achieved by individual outputs calibrated specifically using time series directly related to such output (e.g., when modelled soil moisture is calibrated using soil moisture observations; Figure 5). The decreased performance was generally greater in the forest site, though the performance depreciation was small or nonsignificant (at 95% confidence) for SWC1, SWC2, SWC3, temperature differences, and transpiration rate (in general

$\Delta\text{RMSE} < 11\%$ ;  $\Delta\text{MAE} < 8\%$ ;  $\Delta\text{Pearson} < 0.15$ ). LAI and biomass production ( $\Delta\text{MAE} = 20\%$  and  $17\%$ , respectively) clearly had a higher degradation of performance during global calibration. Specifically, for those variables, the individual calibrations led to a very different selection of different posterior range of values for allocation and turnover parameters (not shown here) compared with the global calibration, indicating that they had strong interactions with other parameters in the water and energy modules. For the grassland, the depreciation in the global calibration was most marked for SWC1 and SWC3. The validation of the model against soil moisture measurements in 2013 produced similar performance measures to calibration; indeed, these were sometimes better, probably because the validation period was shorter and did not contain the more extreme wetter and drier spells of the longer calibration time series (Figure 5). Exceptions were SWC1 in the forest and SWC3 in the grassland.

## 4.2 | Simulation of energy, hydrological, and biomass components

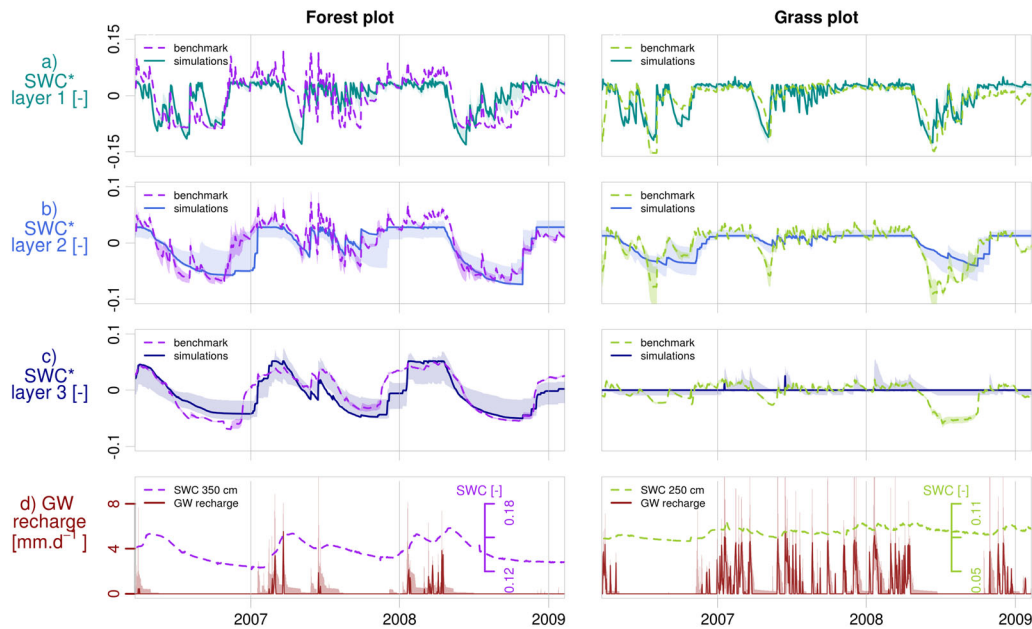
The short term and seasonal dynamics of soil surface temperatures were generally represented with good accuracy for the forest and grassland plots, though there was a slight overestimation at both plots during the early growing season, and an underestimation at the forest plot in late summer (Figure 6a,b). The high fidelity with which the model represented surface temperatures also captured the nuanced contrasts between the forest and grass plots (Figure 6c), reproducing higher growing season surface temperatures in the grass plot at an accuracy of  $<1^\circ\text{C}$ .

Figure 7 shows the centred soil water dynamics of the simulations ( $\text{SWC}^* = \text{SWC} - \text{mean}[\text{SWC}]$ ); plotting this way overcomes the heterogeneity in measured soil moisture and the difficulty comparing the calibrated layer thickness to point measurements without any serious bias. In general, the simulations satisfactorily reproduce the seasonal variability, though increased variation in the ensemble results is evident with increasing depth in the forest. Also, the high frequency dynamic is damped in the upper two layers especially for the forest soils and the third layer at both sites. This relative damping is partly associated with the different volumes over which the model and the observations integrate soil moisture. The larger volume of the model



**FIGURE 6** Simulated soil surface temperature (purple and green) plotted and observed soil surface temperature (black) at forest (a) and grass (b) plots. Soil surface temperature contrast between the plots (c)





**FIGURE 7** Imulation of the soil water content on the first, second, and third layer at both sites. Best simulated and confidence interval of the 15 best simulated  $SWC_i^* = SWC_i - \text{mean}(SWC_i)$ , against the the observed unbiased  $SWC_o^* = SWC_o - \text{mean}(SWC_o)$ ; dashed line). Also simulated groundwater (GW) recharge compared with the SWC observation in deep layer (250 and 350 cm in grassland and forest site). The depths of soil layers are calibrated, so vary in simulations as follows: Layer 1 = 0 to 0.16–0.29 m (forest): 0 to 0.2–0.29 m (grassland). Layer 2 = 0.16–0.29 to 0.37–0.97 m (forest): 0.2–0.29 to 0.57–0.97 m (grassland). Layer 3 = 0.37–0.97 to 1.5 m (forest): 0.57–0.97 to 1.5 m (grassland)

layer tends to damp high frequency dynamics related to local, rapid, and preferential movement of a wetting front which may be captured by point measurements. The soil parameters of saturated hydraulic conductivity and leakance to groundwater were most sensitive in the model, followed by the depth of the upper soil layer (L1) and the Brooks and Corey porosity index (Table S2; Figures S2 and S3).

To further verify the modelled soil water dynamics, we compared the groundwater recharge flux simulated at 150 cm in the model, with the deepest soil moisture measurements (not used in the model) at 250 cm in the grassland and 350 cm in the forest (Figure 7d). In the forest site, both modelled flux and measured soil moisture variability showed good agreement and exhibited much more marked seasonality than the grassland site. In the latter, recharge was higher and was simulated during the wet summer of 2007. There is a time lag of a few weeks in the measured response at the forest (compared with the modelled flux) which is consistent with the greater observation depth (3.5 m compared with 1.5 m).

Calibrated LAI dynamics for the forest plot were within the range broadly consistent with measured seasonal variations (Figure 8). The ranges of LAI variations in the forest and grass plots are  $\sim 4$  and  $\sim 1.0$ , respectively. Average LAI for the grassland site was about 4.4,

which is slightly high for temperate grasslands and may overestimate interception (Munier et al., 2018). In the forest plot, the high LAI increase during the wet summer of 2007, and the unrealistic limited decline during the winter seasons was also notable, which seems to reflect excessive allocation to leaves when moisture is not limiting. This is not consistent with the direct measurement of leaf and needle fall (Table 3) nor with the observed seasonal LAI dynamic (Figure 8), which are unrelated to the variable climatic conditions. This is likely explained by the high sensitivity of biomass allocation in the model to many parameters and may account for why there is a trade-off in the global calibration between biomass production and LAI dynamics. The average modelled above-ground forest biomass production underestimates measured values by  $\sim 10\text{--}30\%$  (Table 3). However, results are broadly consistent between years, and the simulation confidence interval brackets the observation values (Figure S1). Notice that leaf allocation is very consistent between years; however, observation of fruit production shows high variability, suggesting that the stem and fruit pool might be a buffer in the model or capture phenological interannual dynamics unrelated to climate (Lebourgeois et al., 2018), and these detailed physiological aspects are not captured by the model.

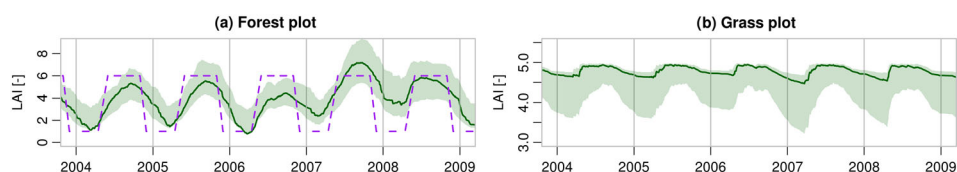


**FIGURE 8** Leaf area index (LAI) simulations over the forest (a) and grass (b) plot: best simulation (solid green line); range of values of the 15 best simulations (green interval); LAI benchmark based on measured maximum and minimum values in the forest plot (purple dashed line)

**TABLE 3** Annual biomass production in the different pools: leaves and needles, fruits production, and stems: from Schulte-Bisping et al. (2012; OBS) and simulation results (SIM)

	Leaves + needles losses (OBS)	Leaves + needles losses (SIM)	Fruits production (OBS)	Stem growth (OBS)	Stem growth + fruits production (SIM)
2004	193	134 ± 49	205	167	268 ± 83
2005	185	170 ± 63	83		301 ± 93
2006	202	145 ± 44	101		232 ± 81
2007	192	142 ± 81	170		401 ± 124
2008	195	166 ± 51	109		287 ± 98

The modelled transpiration rates in the forest have a high range but measured values in the year available are generally bracketed by the spread of simulations, though slight overprediction in the early season and underprediction in midsummer is evident (Figure 9). The simulated grass transpiration rates are lower, especially in the growing season, but the dynamic simulated is similar to the forest (correlation coefficient = 0.85). The model also captures well the transpiration rate decrease in July–August related to the general decrease on soil water availability. For the vegetation parameters, water efficiency, stomatal conductance, and stomatal sensitivity to air pressure and soil wetness were all sensitive (Figures S2 and S3), along with the root and stem allocation factors, and the associated sensitivity of LAI. As expected, the root depth distribution parameters were sensitive for both sites as well as the maximum leaf turnover for the forest plot.

### 4.3 | Water balance for forest and grass plots

Averaged over 11 years, the most marked modelled water balance differences between the two sites were clearest in the higher interception losses from the forest site (though the high LAI and often low intensity rainfall still results in substantial grassland interception; Table 4). Transpiration and evaporation losses were also higher,

though the differences with the grassland were smaller. Consequently, average groundwater recharge under the forest was roughly a third of that under grassland (73 mm compared with 225 mm), mostly due to the trade-off with interception and higher transpiration. Figure 10 shows the seasonality of the main components of the mass balance, with indication of the model uncertainty. The model simulations show consistent higher forest interception losses (especially in summer and autumn [June–October]), higher forest soil evaporation rate (mostly from the spring months [March–May]), and higher groundwater recharge under the grassland, which is especially concentrated during

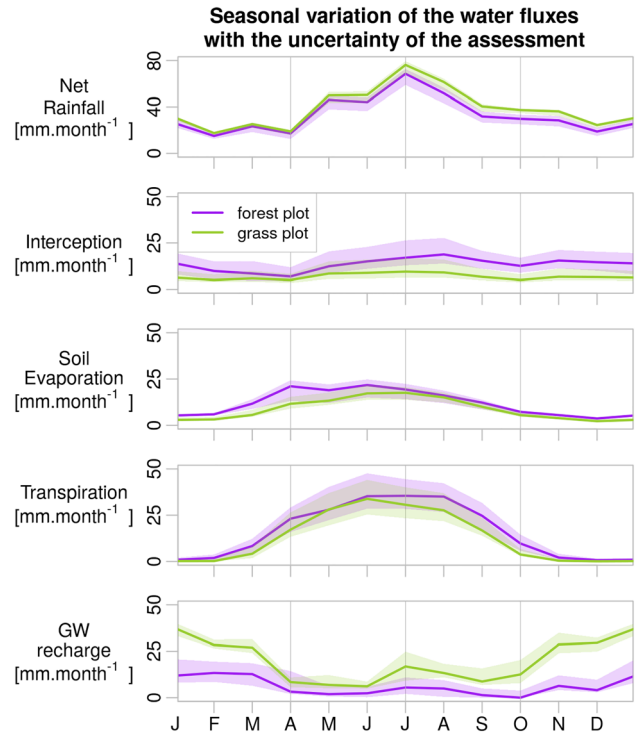


**FIGURE 10** Seasonal averages of the fluxes over the 2004–2014 years, with uncertainty related to model calibration (q5th and q95th of the 15 best simulations)

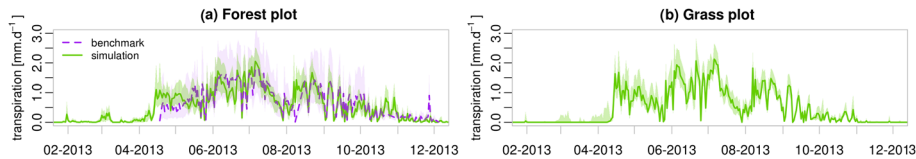


**FIGURE 9** Transpiration rates simulated over one growing season. Comparison in the forest plot to the sapflow measurements

**TABLE 4** Modelled water balance from ECH<sub>2</sub>O-iso

	Interception		Soil evaporation		Transpiration		GW recharge	
	mm	%	mm	%	mm	%	mm	%
Forest	163 ± 31	29 ± 4.0	152 ± 21	25 ± 6.4	210 ± 55	34 ± 3.5	73 ± 67	12 ± 8.3
Grass	104 ± 7	16 ± 2.7	111 ± 14	19 ± 4.0	172 ± 22	29 ± 4.6	225 ± 105	36 ± 10.4

Note. Average yearly assessment with interannual variation (over the period 2004–2014).

Abbreviation: GW, groundwater.

the winter months, but unlike in the forest plot, it can also be high in the summer.

Although the model seems to be successfully partitioning overall “green” and “blue” water fluxes, there is significant uncertainty regarding the allocation of soil evaporation and transpiration in the forest. As a result, forest soil evaporation seems too high, especially in the early spring. Evaporation is sensitive to the trajectory of the modelled LAI, as the slow increase in early growing season allows energy to reach the forest floor and drive evaporative cooling, which is further exacerbated by the cooling effect of the soil temperature as a calibration constraint.

In the grassland plot, groundwater recharge exhibits the greatest interannual variability (standard deviation of  $\pm 105$  mm), with low variation in modelled interception, transpiration, and soil evaporation rates (Table 4). Although groundwater recharge also has the greatest interannual variability in the forest plot (standard deviation  $\pm 67$  mm), variability in transpiration ( $\pm 55$  mm) is similar and high, depending upon the balance between soil moisture availability and atmospheric demand.

#### 4.4 | Storage-flux-mixing interactions in $\text{Ech}_2\text{O}$ -iso: Insights from chloride tracing

Chloride fluxes were simulated using the calibrated model as an independent check on the model's skill in capturing the internal hydrological function of the forest plot. Chloride inputs were routed through the three model layers assuming full mixing in each layer and allowing evapoconcentration from evaporation and transpiration uptake. Chloride inputs were greatest in the winter (typically between November and February) when air masses are more likely to have an oceanic origin, though this can vary between years (e.g., high inputs in the winter of 2006/2007 and low inputs in the winter of 2005/2006; Figure 11). High winter chloride inputs propagate rapidly through the soil profile advecting with the wetting fronts at 30 and 50 cm (Figure S4a). In spring and summer, concentrations decline in precipitation and also in the soils, despite evapoconcentration. At depth (120 cm), there was a usually slight lag of a few weeks in the winter peak of Cl and more attenuation of the decrease in concentrations (Figure S4a). However, in general, average concentrations increased with depth as the effects of evaporation and transpiration were apparent. This was difference was particularly marked in summer (Figure S4b).

$\text{Ech}_2\text{O}$ -iso simulates the Cl concentrations in Layer 1 quite well (Figure 11), capturing winter increases and summer decreases and providing further evidence that flux partitioning is accurately captured by the model (at least in terms of the concentration effects of evaporation and transpiration on inputs) and with limited predictive dispersion. However, in Layer 2, although the model captures the seasonal dynamic, the spread of simulated values increases substantially (Figure 11). This likely reflects high uncertainty in the transpiration losses, which have a compensatory effect on recharge, resulting in some parameter sets giving high transpiration losses, which increases

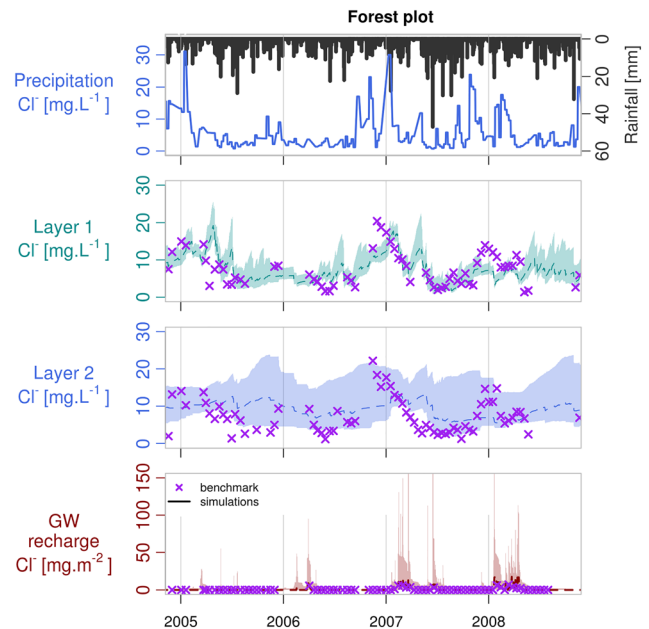


**FIGURE 11** Chloride tracing (15 best simulations) obtained compared with the chloride concentration measured at 30 cm, 50 cm in depth (second and third panels), and chloride fluxes to groundwater (last panel)

Cl concentrations in soil water, whereas some parameter sets give lower concentrations, but higher recharge concentrations through to Layer 3. Consequently, modelled Cl fluxes from the bottom of profile have high uncertainty, though the fluxes estimated from measured data are reproduced quite well for the median parameter values. There is a tendency for some parameter sets to overpredict, which may suggest that Cl concentrations and/or water fluxes are being overestimated in these cases. Despite these uncertainties in the subsoil, the dynamics in Layer 1 and the maintenance of a reasonable mass balance between inputs and outputs adds confidence to overall model results, though emphasizes the increased uncertainties at depth and the need for improvements to the model to constrain this.

#### 4.5 | Estimation of ages of fluxes

The dynamics of water flux ages were broadly similar for both plots (Figure 12), though lower water fluxes beneath the tree canopy resulted in greater ageing of water at depth in the forest (Table 5). The age of evaporated water varied between 1 and 90 days with a mean of around 45 days for both sites. Transpired water was oldest in the forest site, with a mean of 176 days, compared with 87 days in the grassland, reflecting the age of deeper water sources tapped by the influence of greater rooting depths in the distribution calibrated for the forest plot. Generally, ages in the different pools were more-or-less strongly influenced by rainfall distribution at both plots. For the top layer, there was a direct flushing effect on the modelled ages, which declined during and after major rainfall episodes. In the second and third layer, there was significant decrease in water age, mostly when storm events were particularly large (e.g., in the summers

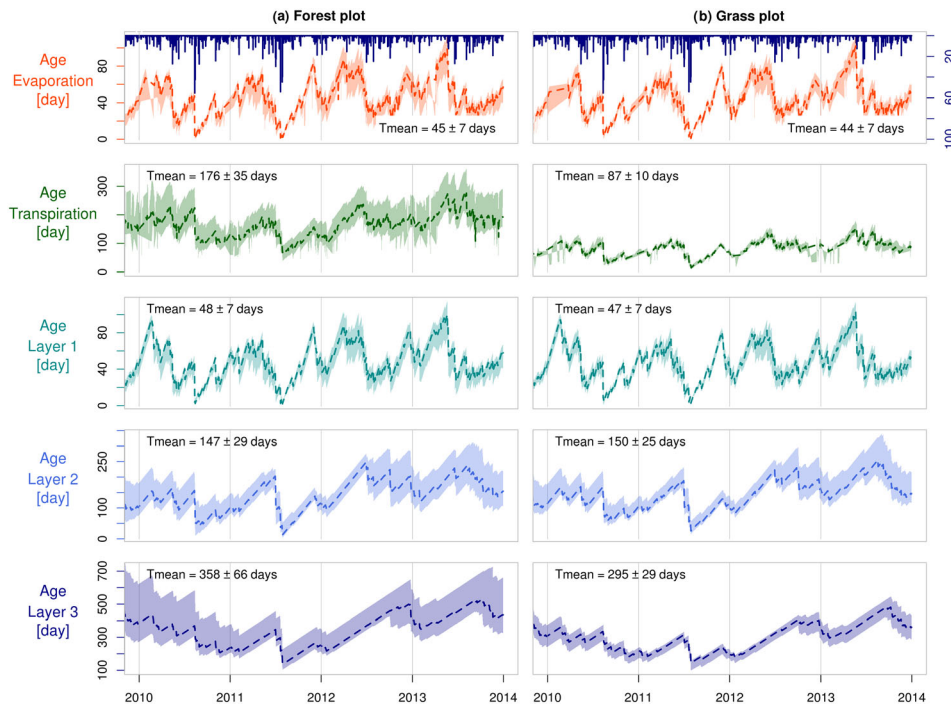


**FIGURE 12** Age of the water fluxes/reservoirs. Confidence interval according to the 15 best simulations, in dashed lined the median age of the 15 simulations

**TABLE 5** Water ages in fluxes: average over the 2004–2014 period

(Day)	Evaporation	Transpiration	L1	L2	L3
Forest	45 ± 8	176 ± 35	48 ± 7	147 ± 29	358 ± 66
Grass	44 ± 7	87 ± 10	47 ± 7	150 ± 25	295 ± 9

Note. Mean and standard variation of the 15 best simulations.

of 2010 and 2011). The ages in the second layer were surprisingly similar, given that we would expect less water turnover in forest plot, though the higher interception and transpiration losses cause slightly greater seasonal variability (about 10 days) in the forest. This effect was enhanced in Layer 3, where the mean ages of water fluxes increased to 358 days in the forest compared with 295 days in the grassland. The ages in L3 exhibited general seasonality, with a tendency to be lower in winter when the main recharge pulses occurred, with ageing during drier summer periods. Nevertheless, as noted above, young water can penetrate to L3 in wet summers such as 2011. Again, uncertainty in the estimated ages was higher in the forest site.

## 5 | DISCUSSION

### 5.1 | Using tracer-aided ecohydrological models to assess land use change impacts

Over the past two decades, ecohydrological models have increasingly enabled us to explicitly consider the role of vegetation in water partitioning and providing a process-based understanding—and means of projecting—the effects of land use change on water resources (e.g., Morán-Tejeda et al., 2015). Tracer-aided ecohydrological models such

as  $\text{Ech}_2\text{O}$ -iso have the potential to enhance this capability by providing a means of conceptualizing the mixing that occurs in water storage—flux interactions, the effect on water ages, and to help constrain the sources of evaporation and plant water use (Kuppel et al., 2018a). By integrating energy exchanges, water fluxes and biomass dynamics, such tracer-aided models also have the potential to provide quantitative insights in to how land cover regulates the interlinkages between water storage—flux—age at different spatial and temporal scales.

Ecohydrologic models tend to be highly parameterized, and the opportunity for insight only exists if a limited number of feasible and consistent model configurations can be identified. Multicriteria calibration and verification of such models can increase the confidence that the dominant ecohydrological processes are being appropriately represented in different landscape compartments and accurately quantified (Kelleher et al., 2017; Kuppel et al., 2018a). Model failure to adequately represent observed processes also provides an opportunity to learn and improve conceptualization (Birkel, Soulsby, & Tetzlaff, 2014; Dunn et al., 2008). The application of  $\text{Ech}_2\text{O}$ -iso to the monitoring site at Lake Stechlin, followed on from a successful catchment-scale application of the model in a wet, boreal catchment in Scottish Highlands (Kuppel et al., 2018a), and the present study provided an opportunity to test the model in a comparative forest/grassland plot-scale study in a more water-limited site and, more importantly, use direct

measures of biomass accumulation and turnover for model calibration. Overall, the model showed good performance in the representation of the different observed components of the energy, water, and (for the forest site) biomass dynamics. The value of including in the calibration process observations pertaining to different components of the ecohydrologic system (water balance, energy balance, and carbon uptake) was very apparent. For instance, it was likely that the model representation of the forest site, where more ecological data were available as a calibration target, was better constrained. The value of the ecological data for the forest site was especially useful given the high sensitivity of most model outputs to vegetation parameters controlling LAI and root distribution, which are not possible to determine from hydrometric data alone, and deeply affect the energy and water balances at seasonal and multiyear scales. For instance, Morales et al. (2005) tested a wide range of hydrological and biogeochemical models across a range of European biomes; the study highlighted the difficulties associated with deciduous forests and the seasonal variations in LAI, and the associated dynamics of interception, throughfall and stem flow.

## 5.2 | Water balance implications

The model simulated a balance of “green” and “blue” water fluxes at the forest site and groundwater recharge rates that were consistent with other investigations at Stechlin (e.g., Pöschke et al., 2018). Although soil moisture had a general seasonality related to winter wetting and summer drying, the permeable nature of the soils along with the occurrence of wet summers with occasionally heavy rainfall, means that recharge can occur all-year round, particularly in the grassland site, and this was well represented by the model.

The partitioning of “green” water fluxes showed wider uncertainty in both the forest and grassland plots. Interception losses simulated for the forest were broadly similar to the differences between measured precipitation and throughfall beneath the forest canopy. There was, however, uncertainty regarding the partitioning of soil evaporation and transpiration in the forest plot. As shown in the results, forest soil evaporation exceeded the evaporation of grasslands between March and May, when soil moisture is still high and the simulated development of the maximum LAI is delayed. The energy not intercepted by canopies due to delayed LAI growth reaches the forest floor and explains the high soil evaporation and the lower transpiration as the LAI increases slowly until August. Increased evaporation due to delayed LAI did not affect the grassland site because LAI from the grassland maintains the LAI relatively high even during periods when grass is not actively growing (hence the high interception). However, evaporation losses are high compared with other literature studies. The higher evaporation may be reflected in the low T:ET ratios for the forest and grassland plots which are only 40 and 44%, respectively. This compares with literature values more typically ~70% (e.g., Fatichi & Pappas, 2017; Good, Noone, & Bowen, 2015; Schlesinger & Jasechko, 2014), whereas 58% was reported by Soubie, Heinesch, Granier, Aubinet, and Vincke (2016) for a similar mixed forest in

Belgium. Thus, despite the effective use of vegetation data to calibrate the model in terms of biomass production and allocation, the data were insufficiently detailed to avoid this uncertainty in the partitioning of soil evaporation and transpiration. Further data may elucidate this; for example, Benyon and Doody (2015) found direct measurement could resolve the partitioning of interception, soil E and T for contrasting forest plots, showing that the relative importance of interception and soil E varied significantly depending on the canopy cover.

Lack of LAI measurements for the grass sward and additional complications introduced by occasional mowing events make it difficult to assess model performance for the grassland plot and how it affects the partition of soil evaporation and transpiration. The upper range of the calibrated grass LAI values in our study are high compared with those usually quoted in the literature. For example, in a global synthesis by Asner, Scurlock, and Hicke (2003), the average range for the mean LAI for grasslands was 0.5–4.2. Nevertheless, LAI values are measurement dependent (e.g., using remote sensing or destructive/non-destructive sampling), and studies on some European grasslands have found values ranging between 3.7 and 7 in alpine pastures (Wohlfahrt et al., 2000; Pasolli et al., 2015). So our model results are within the feasible range and are informative. Regarding the effects of mowing on transpiration, Rose, Coners, and Leuschner (2012) found that mowing one to three times during the growing season had insignificant effect on grassland water use in sites in central Germany, though of course this will affect short-term interception capacity.

## 5.3 | Water age distributions

The simulated differences and dynamics of water ages in the model are comparable with what is reported in the literature. The young water ages (approximately a few months) of water stored in the upper profile of the soils at both plots, which is the main source of evaporation, are similar to those quoted by Sprenger, Tetzlaff, Buttle, Laudon, et al. (2018) for a range of boreal sites. Likewise, the increased age of simulated transpired water from the forest plot, reflecting the greater rooting depths and lower overall water fluxes which age waters deeper in the profile, was also found by Sprenger, Tetzlaff, Buttle, Carey, et al. (2018) and Kuppel et al. (2018a). The ages of deeper recharge integrate these effects, with water draining to Layer 3 being about 20% older in the forest plot, 358 days compared with 295 days in the grassland. Again, these water ages from the bottom of the soil profile are similar in magnitude to others recently reported from elsewhere (e.g., Tetzlaff, Birkel, Dick, Geris, & Soulsby, 2014).

The spread of the modelled age distributions are highest in the forest plot, mainly as a result of the variation in the transpiration estimates. The propagation of the ensemble variation in transpiration to age is also reflected in the simulations of the chloride concentration. The performance of the chloride concentration simulations is best in the upper soil layer, indicating that evapotranspiration fluxes are accurately quantified and that full mixing of the incoming tracer signal is reasonably approximated. However, in L2, the uncertainty over the volume and depth of transpiration explains why the model captures

the general seasonality of the chloride signal reasonably well but does not reproduce the concentrations accurately. However, it should be noted that soil water was sampled by lysimeters under low tension and may not reflect the evaporative signal in finer soil pore waters (Geris, Tetzlaff, McDonnell, & Soulsby, 2017). In contrast, the conceptualization of mixing in  $\text{Ech}_2\text{O}$ -iso tracks the age and tracer concentration of bulk soil water, which includes the water held under higher soil tensions. The effect of this difference may be smaller in the sandy soils of the study site, but even when dry, the residual volumetric SWC in these soils is still 5% and can contribute to the difference between the concentrations in the pool of soil water that is sampled and the concentrations in the bulk soil water represented by the model. Although the celerity of wetting front moving through the soils was evident in the observations and the simulations, the mixing appears to attenuates this modelled signal too rapidly in the deeper soil layers (L2 and L3). A better differentiation of faster and slower flowing water in the model and partial mixing between them would likely improve the chloride simulations (e.g., Sprenger, Tetzlaff, Buttle, Carey, et al., 2018).

#### 5.4 | Implication for using tracer-aided ecohydrological models in land use change studies

Working towards enhancing ecohydrological models through the use of tracers to improve the representation of subsurface mixing and collecting informative data of different types to improve model calibration and parameterization are important goals to refine our models and assess the hydrological implications of land use change under projected climate change scenarios. However, advancing these agenda is predicated on the idea that we know what aspects of the model need to be improved and what data collection efforts should be prioritized. Models can inform these aspects (Peters, Freer, & Beven, 2003). For instance, the excessive damping of the chloride signal indicates that our model needs to incorporate partial or differentiated mixing of faster and slower zones of water movement in the soil (Sprenger, Tetzlaff, Buttle, Carey, et al., 2018). This also provides a basis for better apportioning of the pools of soil water that contribute to evaporation and transpiration and permits a more meaningful comparison with the water compositions sampled by lysimeters.

In addition to better tracer data, improved ecological data sets that represent seasonal to longer term processes are critical to improve the calibration of model components that simulate changes in plant biomass with critical hydrological feedbacks at interannual to decadal timescales. Acquisition of biomass data during measurement campaigns has only recently become common in the hydrologic community. Measurements of the forest LAI over the growing season are probably one of the most important measurements and are relatively common, but additional measurements on root distribution, stem growth, or total biomass are also critical and less common.

As in many modelling studies, this investigation leverages data sets collected for other purposes. Often these data sets provide key long-term historical information; however, they are often not optimal to inform models because the campaigns were not been specifically

designed for this purpose. It is clear that as the fields of ecohydrological and tracer-aided modelling mature, careful planning of data acquisition to best enhance model development and testing is necessary. In the future, such coevolution may facilitate more rapid advances in our understanding and ability to accurately predict the hydrological impacts of land use change. This is a priority for work planned in the drought-sensitive study area of Brandenburg, where the effects of climate change, and predicted warmer, drier summers, may result in scarcity of water resources in future (Lischeid & Nathkin, 2011). More accurate ecohydrological modelling is needed to inform decision making on how different land use scenarios, in terms of the balance of forest and nonforest cover, will involve trade-offs in terms of water availability and other ecosystem services.

## 6 | SUMMARY AND CONCLUSION

We applied a process-based ecohydrological model ( $\text{Ech}_2\text{O}$ -iso) to compare the effects of land cover on water partitioning and associated flux ages under temperate beech forest and grassland on podzolic, sandy soils at Lake Stechlin in Germany. Multicriteria calibration, based on measures of the energy balance, hydrological function, and biomass accumulation, resulted in generally good simulations of surface energy exchange, SWC, transpiration, and biomass production. The model results showed that the forest used more water than the grassland from the 620 mm of average annual precipitation. On average, "green" water fluxes from interception, transpiration, and evaporation were 88% of precipitation inputs under beech forest, compared with 63% under grassland. As a result, groundwater recharge was greatly enhanced under grassland at 37% of precipitation compared with 12% for forest. The model also tracked the ages of water in the different fluxes. In shallow soil horizons, the average ages of soil water fluxes and evaporation were similar in both plots (~1.5 months), though transpiration and groundwater recharge were older under forest (~6 months compared with 3 months for transpiration and ~12 months compared with ~10 months for groundwater). Flux tracking with Cl tracers provided independent support for the modelling results, though it also highlighted effects of uncertainties in the model. To realize the potential for tracer-aided ecohydrological models in land use change studies, further improvements in the conceptualization of soil water mixing and carefully planned data acquisition on biomass dynamics seems the highest priorities for more reliable predictions.

## ACKNOWLEDGMENTS

The authors would like to acknowledge research funding from the European Research Council (project GA 335910 VeWa). M. Maneta acknowledges support from the U.S. National Science Foundation (project GSS 1461576). C. S. is grateful to the Leibniz IGB Berlin for a Senior Research Fellowship. We also thank Umweltbundesamt (UBA) for providing the climate data.

## DATA AVAILABILITY STATEMENT

The data that support the findings of this study are available from the corresponding author upon reasonable request.

## ORCID

Audrey Douinot  <https://orcid.org/0000-0001-9824-0528>

Doerthe Tetzlaff  <https://orcid.org/0000-0002-7183-8674>

Sylvain Kuppel  <https://orcid.org/0000-0003-3632-2100>

Chris Soulsby  <https://orcid.org/0000-0001-6910-2118>

## REFERENCES

- Amogu, O., Esteves, M., Vandervaere, J.-P., Abdou, M. M., Panthou, G., Rajot, J.-L., ... Descroix, L. (2015). Runoff evolution due to land-use change in a small Sahelian catchment. *Hydrological Sciences Journal*, 60(1), 78–95. <https://doi.org/10.1080/02626667.2014.885654>
- Archer, D. R. (2007). The use of flow variability analysis to assess the impact of land use change on the paired Plynlimon catchments, mid-Wales. *Journal of Hydrology*, 347(3–4), 487–496. <https://doi.org/10.1016/j.jhydrol.2007.09.036>
- Asner, G. P., Scurlock, J. M. O., & Hicke, J. A. (2003). Global synthesis of leaf area index observations: Implications for ecological and remote sensing studies. *Global Ecology and Biogeography*, 12, 191–205. <https://doi.org/10.1046/j.1466-822X.2003.00026.x>
- Baldocchi, D. D., Xu, L., & Kiang, N. (2004). How plant functional-type, weather, seasonal drought, and soil physical properties alter water and energy fluxes of an oak–Grass savanna and an annual grassland. *Agricultural and Forest Meteorology*, 123, 13–39. <https://doi.org/10.1016/j.agrformet.2003.11.006>
- Benettin, P., Kirchner, J. W., Rinaldo, A., & Botter, G. (2015). Modeling chloride transport using travel time distributions at Plynlimon, Wales. *Water Resources Research*, 51(5), 3259–3276. <https://doi.org/10.1002/2014WR016600>
- Benyon, R. G., & Doody, T. M. (2015). Comparison of interception, forest floor evaporation and transpiration in *Pinus radiata* and *Eucalyptus globulus* plantations. *Hydrological Processes*, 29(6), 1173–1187. <https://doi.org/10.1002/hyp.10237>
- Bergel, D. (1973). *Massentafeln für Nordwestdeutschland: 1, Buche, Fichte, Europäische Lärche, Japanische Lärche, Douglasie*. Göttingen: Niedersachsen Forstl. Versuchsanst. Abt. Waldwachstum.
- Bergström, I., Mäkelä, K., Starr, M., Rask, M., Holopainen, A., Karusalmi, A., Niinistö, R., Tammi, J., Arvola, L. & Keskitalo, (2003). 5.4 Report on national ICP IM activities in Germany, wge, Page 54.
- Beven, K. (2006). A manifesto for the equifinality thesis. *Journal of Hydrology*, 320, 18–36. <https://doi.org/10.1016/j.jhydrol.2005.07.007>
- Beven, K., & Binley, A. (1992). The future of distributed models: Model calibration and uncertainty prediction. *Hydrological Processes*, 6, 279–298. <https://doi.org/10.1002/hyp.3360060305>
- Birkel, C., Soulsby, C., & Tetzlaff, D. (2014). Developing a consistent process-based conceptualization of catchment functioning using measurements of internal state variables. *Water Resources Research*, 50, 3481–3501. <https://doi.org/10.1002/2013WR014925>
- Birkel, C., Soulsby, C., & Tetzlaff, D. (2011). Modelling catchment-scale water storage dynamics: Reconciling dynamic storage with tracer-inferred passive storage. *Hydrological Processes*, 25(25), 3924–3936. <https://doi.org/10.1002/hyp.8201>
- Bossel, H. (1996). Treedyn3 forest simulation model. *Ecological Modelling*, 90, 187–227. [https://doi.org/10.1016/0304-3800\(95\)00139-5](https://doi.org/10.1016/0304-3800(95)00139-5)
- Brüning, C., Graf, A. & Nützmann G. (2003). Bodenhydrologische Meßstellen Neuglobsow/Stechlinsee (UN/ECE-Integrated Monitoring). *Institut für Gewässerökologie und Binnenfischerei, Abteilung Ökohydrologie, Überarbeitete Fassung März 2003*.
- Casper, S. J. (Ed.) (2012). *Lake Stechlin: A temperate oligotrophic lake* (Vol. 58). Berlin/Heidelberg, Germany: Springer Science & Business Media. <https://doi.org/10.1007/978-94-009-5506-6>
- Chapin, F. S., Matson, P. A., & Vitousek, P. M. (2011). *Principles of terrestrial ecosystem ecology*. New York: Springer. <https://doi.org/10.1007/978-1-4419-9504-9>
- Dee, D. P., Uppala, S. M., Simmons, A. J., Berrisford, P., Poli, P., Kobayashi, S., ... Vitart, F. (2011). The ERA-Interim reanalysis: Configuration and performance of the data assimilation system. *Quarterly Journal of the Royal Meteorological Society*, 137, 553–597. <https://doi.org/10.1002/qj.828>
- Dieffenbach-Fries, H., Hofmann, R., & Schleyer, R. (2003). Report on national ICP IM activities in Germany 2002–2003. In S. Kleemola, & M. Forsius (Eds.), *12th Annual Report 2003*. UN ECE ICP Integrated Monitoring (Vol. 637) (pp. 54–58). Helsinki, Finland: The Finnish Environment Institute.
- Dorau, K., Gelhausen, H., Esplör, D., & Mansfeldt, T. (2015). Wetland restoration management under the aspect of climate change at a mesotrophic fen in Northern Germany. *Ecological Engineering*, 84, 84–91. <https://doi.org/10.1016/j.ecoleng.2015.07.017>
- Dunn, S. M., Freer, J., Weiler, M., Kirkby, M. J., Seibert, J., Quinn, P. F., ... Soulsby, C. (2008). Conceptualization in catchment modelling: Simply learning? *Hydrological Processes*, 22, 2389–2393. <https://doi.org/10.1002/hyp.7070>
- Evaristo, J., Jasechko, S., & McDonnell, J. J. (2015). Global separation of plant transpiration from groundwater and streamflow. *Nature, Nature Publishing Group*, 525(7567), 91–94. <https://doi.org/10.1038/nature14983>
- Fagerli, H., & Aas, W. (2008). Trends of nitrogen in air and precipitation: Model results and observations at EMEP sites in Europe, 1980–2003. *Environmental Pollution*, 154, 448–461. <https://doi.org/10.1016/j.envpol.2008.01.024>
- Fatichi, S., Ivanov, V. Y., & Caporali, E. (2012). A mechanistic ecohydrological model to investigate complex interactions in cold and warm water-controlled environments: 1. Theoretical framework and plot-scale analysis. *Journal of Advances in Modeling Earth Systems*, 4(2). <https://doi.org/10.1029/2011MS000086>
- Fatichi, S., & Pappas, C. (2017). Constrained variability of modeled T:ET ratio across biomes. *Geophysical Research Letters*, 44, 6795–6803. <https://doi.org/10.1002/2017GL074041>
- Fatichi, S., Pappas, C., & Ivanov, V. Y. (2016). Modeling plant–water interactions: An ecohydrological overview from the cell to the global scale. *WIREs Water*, 3, 327–368. <https://doi.org/10.1002/wat2.1125>
- Frei, C., Schöll, R., Fukutome, S., Schmidli, J., & Vidale, P. L. (2006). Future change of precipitation extremes in Europe: Intercomparison of scenarios from regional climate models. *Journal of Geophysical Research-Atmospheres*, 111, Issue D6, D06105. <https://doi.org/10.1029/2005JD005965>
- García-Ruiz, J. M., Regúes, D., Alvera, B., Lana-Renault, N., Serrano-Muela, P., Nadal-Romero, E., ... Arnáez, J. (2008). Flood generation and sediment transport in experimental catchments affected by land use changes in the central Pyrenees. *Journal of Hydrology*, 356(1–2), 245–260. <https://doi.org/10.1016/j.jhydrol.2008.04.013>
- Geris, J., Tetzlaff, D., McDonnell, J. J., & Soulsby, C. (2017). Spatial and temporal patterns of soil water storage and vegetation water use in humid northern catchments. *Science of the Total Environment*, 595, 486–493. <https://doi.org/10.1016/j.scitotenv.2017.03.275>

- Ginzel, G., Kaboth, U., (1999). Hydrogeologisches Gutachten NSG Stechlin. IGB 15 pages, unpublished.
- Good, S. P., Noone, D., & Bowen, G. (2015). Hydrologic connectivity constrains partitioning of global terrestrial water fluxes. *Science, American Association for the Advancement of Science*, 349, 175–177. <https://doi.org/10.1126/science.aaa5931>
- Gupta, H. V., Kling, H., Yilmaz, K. K., & Martinez, G. F. (2009). Decomposition of the mean squared error and NSE performance criteria: Implications for improving hydrological modelling. *Journal of Hydrology*, 377, 80–91. <https://doi.org/10.1016/j.jhydrol.2009.08.003>
- Huisman, J., Breuer, L., Bormann, H., Bronstert, A., Croke, B., Frede, H.-G., ... Willems, P. (2009). Assessing the impact of land use change on hydrology by ensemble modeling (LUCHEM) III: Scenario analysis. *Advances in Water Resources*, 32, 159–170. <https://doi.org/10.1016/j.advwatres.2008.06.009>
- Istanbulluoglu, E., Wang, T., & Wedin, D. A. (2012). Evaluation of ecohydrologic model parsimony at local and regional scales in a semiarid grassland ecosystem. *Ecohydrology*, 5, 121–142. <https://doi.org/10.1002/eco.211>
- Ivanov, V. Y., Bras, R. L., & Vivoni, E. R. (2008). Vegetation-hydrology dynamics in complex terrain of semiarid areas: 1. A mechanistic approach to modeling dynamic feedbacks. *Water Resources Research*, 44(3). <https://doi.org/10.1029/2006WR005588>
- Jencso, K. G., & McGlynn, B. L. (2011). Hierarchical controls on runoff generation: Topographically driven hydrologic connectivity, geology, and vegetation. *Water Resources Research*, 47(11), W11527. <https://doi.org/10.1029/2F2011WR010666>
- Jolly, W. M., & Running, S. W. (2004). Effects of precipitation and soil water potential on drought deciduous phenology in the Kalahari. *Global Change Biology*, 10(3), 303–308. <https://doi.org/10.1046/j.1365-2486.2003.00701.x>
- Kelleher, C., McGlynn, B., & Wagener, T. (2017). Characterizing and reducing equifinality by constraining a distributed catchment model with regional signatures, local observations, and process understanding. *Hydrology and Earth System Sciences*, 21, 3325–3352. <https://doi.org/10.5194/hess-21-3325-2017>
- Klaus, J., Chun, K. P., McGuire, K. J., & McDonnell, J. J. (2015). Temporal dynamics of catchment transit times from stable isotope data. *Water Resources Research*, 51, 4208–4223. <https://doi.org/10.1002/2014WR016247>
- Kuppel, S., Tetzlaff, D., Maneta, M. P., & Soulsby, C. (2018a). What can we learn from multi-data calibration of a process-based ecohydrological model? *Environmental Modelling & Software*, 101, 301–316. <https://doi.org/10.1016/j.envsoft.2018.01.001>
- Kuppel, S., Tetzlaff, D., Maneta, M. P., & Soulsby, C. (2018b). EcH\_2O-iso 1.0: water isotopes and age tracking in a process-based, distributed ecohydrological model. *Geoscientific Model Development*, 11, 3045–3069. <https://doi.org/10.5194/gmd-11-3045-2018>
- Landsberg, J. J., & Waring, R. H. (1997). A generalised model of forest productivity using simplified concepts of radiation-use efficiency, carbon balance and partitioning. *Forest Ecology and Management*, 95, 209–228. [https://doi.org/10.1016/S0378-1127\(97\)00026-1](https://doi.org/10.1016/S0378-1127(97)00026-1)
- Lebourgeois, F., Delpierre, N., Dufrêne, E., Cecchini, S., Macé, S., Croisé, L., & Nicolas, M. (2018). Assessing the roles of temperature, carbon inputs and airborne pollen as drivers of fructification in European temperate deciduous forests. *European Journal of Forest Research*, Springer, 137(3), 349–365. <https://doi.org/10.1007/s10342-018-1108-1>
- Lischeid, G., & Nathkin, M. (2011). The potential of land-use change to mitigate water scarcity in northeast Germany—A review. *DIE ERDE, Journal of the Geographical Society of Berlin*, 142, 97–113.
- Llorens, P., & Domingo, F. (2007). Rainfall partitioning by vegetation under Mediterranean conditions. A review of studies in Europe. *Journal of Hydrology*, 335(1–2), 37–54. <https://doi.org/10.1016/j.jhydrol.2006.10.032>
- Lozano-Parra, J., Maneta, M. P., & Schnabel, S. (2014). Climate and topographic controls on simulated pasture production in a semiarid Mediterranean watershed with scattered tree cover. *Hydrology and Earth System Sciences*, 18, 1439–1456. <https://doi.org/10.5194/hess-18-1439-2014>
- Maneta, M. P., & Silverman, N. L. (2013). A spatially distributed model to simulate water, energy, and vegetation dynamics using information from regional climate models. *Earth Interactions*, 17, 1–44. <https://doi.org/10.1175/2012EI000472.1>
- Mays, L. W. (2010). *Water resources engineering* (p. 928). New York: John Wiley & Sons.
- McDonnell, J. J. (2014). The two water world's hypothesis: Ecohydrological separation of water between streams and trees? *Wiley Interdisciplinary Reviews Water*, 1, 323–329. <https://doi.org/10.1002/wat2.1027>
- McGuire, K. J., & McDonnell, J. J. (2006). A review and evaluation of catchment transit time modeling. *Journal of Hydrology*, 330(3–4), 543–563. <https://doi.org/10.1016/j.jhydrol.2006.04.020>
- Menzel, A., Sparks, T. H., Estrella, N., Koch, E., Aasa, A., Ahas, R., ... Zust, A. (2006). European phenological response to climate change matches the warming pattern. *Global Change Biology*, 12(10), 1969–1976. <https://doi.org/10.1111/j.1365-2486.2006.01193.x>
- Merz, C., & Pekdeger, A. (2011). Anthropogenic changes in the landscape hydrology of the Berlin-Brandenburg region. *DIE ERDE--Journal of the Geographical Society of Berlin*, 142, 21–39.
- Mirfenderesgi, G., Bohrer, G., Matheny, A. M., Faticchi, S., de Moraes Frasson, R. P., & Schäfer, K. V. R. (2016). Tree level hydrodynamic approach for resolving aboveground water storage and stomatal conductance and modeling the effects of tree hydraulic strategy. *Journal of Geophysical Research - Biogeosciences*, 121, 1792–1813. <https://doi.org/10.1002/2016JG003467>
- Morales, P., Sykes, M. T., Prentice, I. C., Smith, P., Smith, B., Bugmann, H., ... Ogee, J. (2005). Comparing and evaluating process-based ecosystem model predictions of carbon and water fluxes in major European forest biomes. *Global Change Biology*, 11, 2211–2233. <https://doi.org/10.1111/j.1365-2486.2005.01036.x>
- Morán-Tejeda, E., Zabalza, J., Rahman, K., Gago-Silva, A., López-Moreno, J. I., Vicente-Serrano, S., ... Beniston, M. (2015). Hydrological impacts of climate and land-use changes in a mountain watershed: Uncertainty estimation based on model comparison. *Ecohydrology*, 8, 1396–1416. <https://doi.org/10.1002/eco.1590>
- Munier, S., Carrer, D., Planque, C., Camacho, F., Albergel, C., & Calvet, J.-C. (2018). Satellite Leaf Area Index: Global scale analysis of the tendencies per vegetation type over the last 17 years. *Remote Sensing*, 10(3). <https://doi.org/10.3390/rs10030424>
- Nikulín, G., Kjellström, E., Hansson, U., Strandberg, G., & Ullerstig, A. (2011). Evaluation and future projections of temperature, precipitation and wind extremes over Europe in an ensemble of regional climate simulations. *Tellus A: Dynamic Meteorology and Oceanography*, 63(1), 41–55. <https://doi.org/10.1111/j.1600-0870.2010.00466.x>
- Niu, G.-Y., Paniconi, C., Troch, P. A., Scott, R. L., Durcik, M., Zeng, X., ... Goodrich, D. C. (2014). An integrated modelling framework of catchment-scale ecohydrological processes: 1. Model description and tests over an energy-limited watershed. *Ecohydrology*, 7, 427–439. <https://doi.org/10.1002/eco.1362>
- Nützmann, G., Holzbecher, E. & Pekdeger, A. (2003). Evaluation of the water balance of Lake Stechlin with the help of chloride data. *Ergebnisse der Limnologie, Schweizerbart*, Pages 11–23.



- Pasolli, L., Asam, S., Castelli, M., Bruzzone, L., Wohlfahrt, G., Zebisch, M., & Notarnicola, C. (2015). Retrieval of Leaf Area Index in mountain grasslands in the Alps from MODIS satellite imagery. *Remote Sensing of Environment*, *165*, 159–174. ISSN 0034-4257. <https://doi.org/10.1016/j.rse.2015.04.027>
- Peng, C., Liu, J., Dang, Q., Apps, M. J., & Jiang, H. (2002). TRIPLEX: A generic hybrid model for predicting forest growth and carbon and nitrogen dynamics. *Ecological Modelling*, *153*, 109–130. [https://doi.org/10.1016/S0304-3800\(01\)00505-1](https://doi.org/10.1016/S0304-3800(01)00505-1)
- Peters, N. E., Burns, D. A., & Aulenbach, B. T. (2014). Evaluation of high-frequency mean streamwater transit-time estimates using groundwater age and dissolved silica concentrations in a small forested watershed. *Aquatic Geochemistry*, *20*, 183–202. <https://doi.org/10.1007/s10498-013-9207-6>
- Peters, N. E., Freer, J., & Beven, K. (2003). Modelling hydrologic responses in a small forested catchment (Panola Mountain, Georgia, USA): A comparison of the original and a new dynamic TOPMODEL. *Hydrological Processes*, *17*, 345–362. <https://doi.org/10.1002/hyp.1128>
- Peters, N. E., & Ratcliffe, E. B. (1998). Tracing hydrologic pathways using chloride at the Panola Mountain Research Watershed, Georgia, USA. *Water, Air, and Soil Pollution*, *105*, 263–275. <https://doi.org/10.1023/A:1005082332332>
- Porporato, A., Laio, F., Ridolfi, L., & Rodriguez-Iturbe, I. (2001). Plants in water-controlled ecosystems: active role in hydrologic processes and response to water stress. *Advances in Water Resources*, *24*(7), 725–744. [https://doi.org/10.1016/S0309-1708\(01\)00006-9](https://doi.org/10.1016/S0309-1708(01)00006-9)
- Pöschke, F., Nützman, G., Engesgaard, P., & Lewandowski, J. (2018). How does the groundwater influence the water balance of a lowland lake? A field study from Lake Stechlin, north-eastern Germany. *Limnologica*, *68*, 17–25. <https://doi.org/10.1016/j.limno.2017.11.005>
- Remondi, F., Kirchner, J. W., Burlando, P., & Fatichi, S. (2018). Water flux tracking with a distributed hydrological model to quantify controls on the spatio-temporal variability of transit time distributions. *Water Resources Research*, *54*, 3081–3099. <https://doi.org/10.1002/2017WR021689>
- Richter, D. (1997). Das Langzeitverhalten von Niederschlag und Verdunstung und dessen Auswirkungen auf den Wasserhaushalt des Stechlinseegebietes, *Berichte des Deutschen Wetterdienstes*, Volume 201.
- Riediger, J., Breckling, B., Svoboda, N., & Schröder, W. (2016). Modelling regional variability of irrigation requirements due to climate change in Northern Germany. *Science of the Total Environment*, *541*, 329–340. <https://doi.org/10.1016/j.scitotenv.2015.09.043>
- Rose, L., Coners, H., & Leuschner, C. (2012). Effects of fertilization and cutting frequency on the water balance of a temperate grassland. *Ecohydrology*, *5*, 64–72. <https://doi.org/10.1002/eco.201>
- Samek, R. (2000). Hydrogeochemische untersuchungen zur genese des grundwassers im einzugsgebiet des stechlinsees. Master Thesis. Free University Berlin.
- Schlesinger, W. H., & Jasechko, S. (2014). Transpiration in the global water cycle. *Agricultural and Forest Meteorology*, *189–190*, 115–117. <https://doi.org/10.1016/j.agrformet.2014.01.011>
- Schulte-Bisping, H., Beese, F., & Dieffenbach-Fries, H. (2012). C-fluxes and C-turnover of a mature mixed beech and pine stand under increasing temperature at ICP Integrated Monitoring site in Neuglobsow (Brandenburg). *European Journal of Forest Research*, *131*, 1601–1609. <https://doi.org/10.1007/s10342-012-0627-4>
- Simeone, C., Maneta, M. P., Holden, Z. A., Sapes, G., Sala, A., & Dobrowski, S. Z. (2019). Coupled ecohydrology and plant hydraulics modeling predicts ponderosa pine seedling mortality and lower treeline in the US Northern Rocky Mountains. *New Phytologist*, *221*, 1814–1830. <https://doi.org/10.1111/nph.15499>
- Soubie, R., Heinesch, B., Granier, A., Aubinet, M., & Vincke, C. (2016). Evapotranspiration assessment of a mixed temperate forest by four methods: Eddy covariance, soil water budget, analytical and model. *Agricultural and Forest Meteorology*, *228–229*, 191–204. <https://doi.org/10.1016/j.agrformet.2016.07.001>
- Soulsby, C., Birkel, C., Geris, J., Dick, J., Tunaley, C., & Tetzlaff, D. (2015). Stream water age distributions controlled by storage dynamics and nonlinear hydrologic connectivity: Modeling with high-resolution isotope data. *Water Resources Research*, *51*, 7759–7776. <https://doi.org/10.1002/2015WR017888>
- Speich, M., Lischke, H., Scherstjanoi, M., & Zappa, M. (2016). FORHYCS: A coupled, spatially distributed eco-hydrological model for assessing climate and land use change impact in Switzerland at landscape scale, *EGU General Assembly Conference Abstracts*, Volume 18, 12988.
- Sprenger, M., Tetzlaff, D., Buttle, J., Carey, S. K., McNamara, J. P., Laudon, H., ... Soulsby, C. (2018). Storage, mixing, and fluxes of water in the critical zone across northern environments inferred by stable isotopes of soil water. *Hydrological Processes*, *32*, 1720–1737. <https://doi.org/10.1002/hyp.13135>
- Sprenger, M., Tetzlaff, D., Buttle, J., Laudon, H., Leistert, H., Mitchell, C. P. J., ... Soulsby, C. (2018). Measuring and modelling stable isotopes of mobile and bulk soil water. *Vadose Zone Journal*, *Soil Science Society of America*, *17*(1), 1–18, 170149. <https://doi.org/10.2136/VZJ2017.08.0149>
- Tague, C. L., & Band, L. E. (2004). RHESSys: Regional hydro-ecologic simulation system—An object-oriented approach to spatially distributed modeling of carbon, water, and nutrient cycling. *Earth Interactions*, *8*(19), 1–42. [https://doi.org/10.1175/1087-3562\(2004\)8<1:RRHSSO>2.0.CO;2](https://doi.org/10.1175/1087-3562(2004)8<1:RRHSSO>2.0.CO;2)
- Tetzlaff, D., Birkel, C., Dick, J., Geris, J., & Soulsby, C. (2014). Storage dynamics in hydro-pedological units control hillslope connectivity, runoff generation and the evolution of catchment transit time distributions. *Water Resources Research*, *50*, 969–985. <https://doi.org/10.1002/2013WR014147>
- Tetzlaff, D., Soulsby, C., Buttle, J., Capell, R., Carey, S. K., Laudon, H., ... Shanley, J. (2013). Catchments on the cusp? Structural and functional change in northern ecohydrology. *Hydrological Processes*, *27*(5), 766–774. <https://doi.org/10.1002/hyp.9700>
- Thorntwaite, C. W. (1948). An approach toward a rational classification of climate. *Geographical Review*, *American Geographical Society*, *Wiley*, *38*, 55–94. <https://doi.org/10.2307/210739>
- Tørseth, K., Aas, W., Breivik, K., Fjærraa, A. M., Fiebig, M., Hjellbrekke, A. G., ... Yttri, K. E. (2012). Introduction to the European Monitoring and Evaluation Programme (EMEP) and observed atmospheric composition change during 1972–2009. *Atmospheric Chemistry and Physics*, *12*, 5447–5481. <https://doi.org/10.5194/acp-12-5447-2012>
- Trenberth, K., Jones, P. D., Ambenje, P., Bojariu, R., Easterling, D., Klein Tank, A., ... Zhai, P. (2007). Observations: Surface and atmospheric climate change. In *IPCC Fourth Assessment Report: Climate Change 2007. Working Group I: The Physical Science Basis*, chapter 3, intergovernmental panel on climate change (pp. 236–336). Cambridge: Cambridge University Press.
- van Huijgevoort, M. H. J., Tetzlaff, D., Sutanudjaja, E. H., & Soulsby, C. (2016). Using high resolution tracer data to constrain water storage, flux and age estimates in a spatially distributed rainfall-runoff model. *Hydrological Processes*, *30*, 4761–4778. <https://doi.org/10.1002/hyp.10902>
- Villegas, J. C., Dominguez, F., Barron-Gafford, G. A., Adams, H. D., Guardiola-Claramonte, M., Sommer, E. D., ... Huxman, T. E. (2015).

- Sensitivity of ET partitioning to woody cover. *Global Ecology and Biogeography*, 24, 1040–1048. <https://doi.org/10.1111/geb.12349>
- Wang, H., Tetzlaff, D., Dick, J. J., & Soulsby, C. (2017). Assessing the environmental controls on Scots pine transpiration and the implications for water partitioning in a boreal headwater catchment. *Agricultural and Forest Meteorology*, 240, 58–66. <https://doi.org/10.1016/j.agrformet.2017.04.002>
- Wang, L., Good, S. P., & Caylor, K. K. (2014). Global synthesis of vegetation control on evapotranspiration partitioning. *Geophysical Research Letters*, 41, 6753–6757. <https://doi.org/10.1002/2014GL061439>
- Wegehenkel, M. (2009). Modeling of vegetation dynamics in hydrological models for the assessment of the effects of climate change on evapotranspiration and groundwater recharge. *Advances in Geosciences*, 21(1), 109–115. <https://doi.org/10.5194/adgeo-21-109-2009>
- Williams, C. A., Reichstein, M., Buchmann, N., Baldocchi, D., Beer, C., Schwalm, C., ... Schaefer, K. (2012). Climate and vegetation controls on the surface water balance: Synthesis of evapotranspiration measured across a global network of flux towers. *Water Resources Research*, 48(6), W06523. <https://doi.org/10.1029/2F2011WR011586>
- Wohlfahrt, G., Bahn, M., Tappeiner, U., Cernusca, A. & (2000). A model of whole plant gas exchange for herbaceous species from mountain grassland sites differing in land use. *Ecological Modelling*, 125(2–3), 173–201 ISSN 0304-3800. [https://doi.org/10.1016/S0304-3800\(99\)00180-5](https://doi.org/10.1016/S0304-3800(99)00180-5)
- Zhang, S., Yang, H., Yang, D., & Jayawardena, A. W. (2016). Quantifying the effect of vegetation change on the regional water balance within the Budyko framework. *Geophysical Research Letters*, 43, 1140–1148. <https://doi.org/10.1002/2015GL066952>

## SUPPORTING INFORMATION

Additional supporting information may be found online in the Supporting Information section at the end of the article.

**How to cite this article:** Douinot A, Tetzlaff D, Maneta M, Kuppel S, Schulte-Bisping H, Soulsby C. Ecohydrological modelling with EcH<sub>2</sub>O-iso to quantify forest and grassland effects on water partitioning and flux ages. *Hydrological Processes*. 2019;1–18. <https://doi.org/10.1002/hyp.13480>